RSC Advances

This is an *Accepted Manuscript*, which has been through the Royal Society of Chemistry peer review process and has been accepted for publication.

Accepted Manuscripts are published online shortly after acceptance, before technical editing, formatting and proof reading. Using this free service, authors can make their results available to the community, in citable form, before we publish the edited article. This *Accepted Manuscript* will be replaced by the edited, formatted and paginated article as soon as this is available.

You can find more information about *Accepted Manuscripts* in the Information for Authors.

Please note that technical editing may introduce minor changes to the text and/or graphics, which may alter content. The journal's standard Terms & Conditions and the Ethical guidelines still apply. In no event shall the Royal Society of Chemistry be held responsible for any errors or omissions in this *Accepted Manuscript* or any consequences arising from the use of any information it contains.

ROYAL SOCIETY OF CHEMISTRY

www.rsc.org/advances

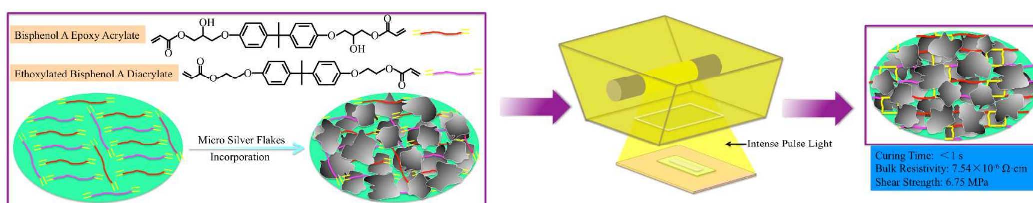

Vinyl ester resin/silver flakes electrically conductive adhesives, combing with intense pulsed light, present ultra-fast photonic curing within a second.

RSC Advances Accepted Manuscript

RSC Advances RSCPublishing

ARTICLE

Cite this: DOI: 10.1039/x0xx00000x

Received 00th January 2012,
Accepted 00th January 2012

DOI: 10.1039/x0xx00000x

www.rsc.org/

Ultra-Fast Photonic Curing Electrically Conductive Adhesives from Vinyl Ester Resin and Silver Flakes for Printed Electronics

Hui-Wang Cui[a,*], Jin-Ting Jiu[a], Nagao Shijo[a], Tohru Sugahara[a], Katsuaki Suganuma[a], Hiroshi Uchida[b] and Kurt A. Schroder[c]

To avoid high temperatures and long curing times, both of which are impractical in the manufacture of flexible printed electronics devices, we fabricated new electrically conductive adhesives using vinyl ester resin and micro silver flakes and introduced an intense pulse of light to cure the adhesives under ambient atmosphere at room temperature. The vinyl ester resin/silver flakes electrically conductive adhesives can absorb intense pulsed light, which initialized the double bonds in the resin to achieve crosslinking and curing successfully. This curing process known as photonic curing can be finished within a second under ambient atmosphere at room temperature over a large area. A typical curing time was 140 ms without any photo sensitizer or photo initiator in the adhesives. The cured conductive adhesives had low bulk resistivity, e.g., 7.54×10^{-6} Ω·cm and high bonding strength, e.g., 6.75 MPa. Thus, the combination of photonic curing and vinyl ester resin/silver flakes electrically conductive adhesives has a great potential for printed electronics, which require low temperature and fast processes based on flexible devices.

Introduction

As an environmentally friendly alternative to lead bearing solders, electrically conductive adhesives (ECAs) have been used widely in manufacturing microelectronics because of the reduced number of processing steps (e.g., elimination of fluxing and reduction of cleaning components), low processing temperatures, which enable use of heat-sensitive and low cost components and substrates, and potentially the capability of fine pitch interconnection.[1,2] Improving mechanical strength, increasing electrical conductivity, shortening curing time, raising production efficiency, etc., have been the hot research topics for the development and application of ECAs.[2] Copper particles,[3,4] micro silver flakes,[5,6] nano silver rods,[7,8] functionalized carbon nanotubes,[9-11] silver plated nano graphite sheets,[12,13] nano silver wires,[14,15] and nano hexagonal boron nitride particles[16,17] have been used as electrically conductive fillers to increase electrical conductivity; epoxy,[10,11] silicone resin,[18,19] polyimide resin,[20,21] phenol-formaldehyde resin,[22,23] polyurethane,[24,25] and acrylic resin[26,27] together with diluent,[6,28] curing agent,[6,28] crosslinker,[29,30] coupling agent,[6,28] preservative,[31,32] toughening agent,[33,34] thixotropic agent,[35] photo sensitizer, and photo initiator[36,37] as matrix resin for improving mechanical strength and shortening curing time. Most of these ECAs are cured by heat at 120－150 °C in 30－60 min or by ultraviolet rays in several to tens of minutes. However, the heat curing and ultraviolet ray curing conditions, due to the limitations of high temperature and long curing time, are unacceptable if ECAs are to be used in printed electronics, which need low temperatures and short processing times.

For printed electronics, many high-speed sintering systems have been developed, such as electrical,[38,39] laser,[40,41] microwave,[42,43] photonic curing,[44,45] also refereed to as flash light[46,47] or intense pulsed light,[48-50] to replace conventional heat sintering process taking over a few minutes to a few hours. Among them, the photonic curing technique can sinter and cure materials in an ambient atmosphere over a large area almost instantly–from micro seconds to a few seconds. This technique plays an important role in roll-to-roll printing process of rapid and eco-friendly electronic device manufacturing and can achieve higher throughput than any other sintering technique in printed electronics. There are no reports on using photonic curing to cure ECAs so far because heat curing and ultraviolet ray curing are still the main streams for the application of ECAs. Therefore, in this study, we fabricated the ECAs using a vinyl ester resin and micro silver flakes, and then introduced an intense pulsed light to cure them (Scheme 1); the curing, thermal properties, electrical properties, mechanical properties, and surface morphologies of which we investigated using Fourier transform infrared spectroscopy (FTIR), differential scanning calorimeter (DSC), thermogravimetric-differential thermal analysis (TG-DTA), field emission scanning electron microscopy (FE-SEM), four-point probe method, nanoindentation, and shear test.

RSC Advances Accepted Manuscript

This journal is © The Royal Society of Chemistry 2013

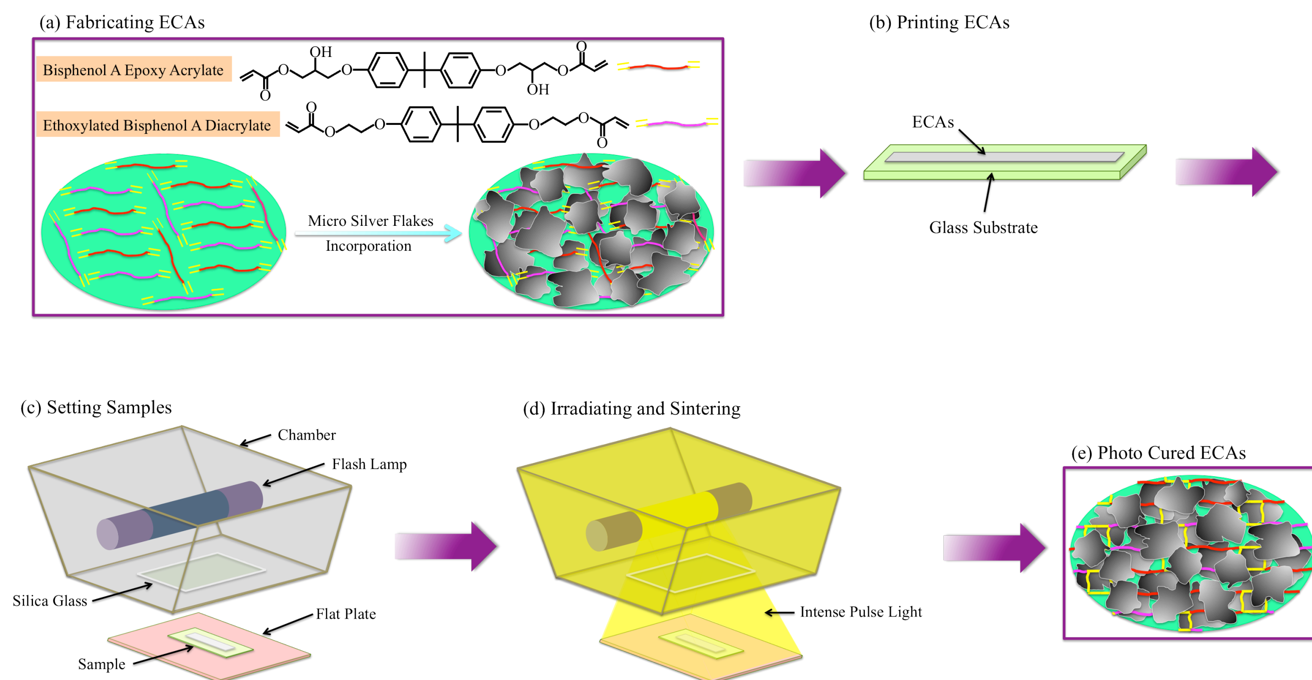

Scheme 1 Preparation of ultra-fast photonic curing ECAs: (a) fabricating ECAs, (b) printing ECAs, (c) setting samples, (d) irradiating and sintering, and (e) photonically cured ECAs

Experiments

Samples

The ECAs consisted of a matrix resin and electrically conductive fillers. The matrix resin was a Ripoxy SP-1507 vinyl ester resin from Showa Denko, Chibaken, Japan, which was a bisphenol A epoxy acrylate diluted by ethoxylated bisphenol A diacrylate [Scheme 1(a)]. The viscosity was 18700 mPa·s (25 °C). Electrically conductive fillers were AgC-239 micro silver flakes [Figure 1(a)] from Fukuda Metal Foil & Powder Co., Ltd., Kyoto, Japan. The size was 2—15 μm and the thickness around 0.5 μm. The weight percentages of micro silver flakes were 80%, 85%, and 90% in ECAs, respectively. The ECAs were named as ECAs-80, ECAs-85, and ECAs-90 accordingly. To fabricate these ECAs, micro silver flakes were incorporated into the vinyl ester resin using a THINKY ARV-310 planetary vacuum mixer (THINKY Corporation, Laguna Hills, CA, USA.) under 2000 rpm for 20 min [Scheme 1(a)]. After the fabrication, the ECAs were stored at room temperature for further use. To conduct the photonic curing, the ECAs were printed on glass substrates [Scheme 1(b)], and were then irradiated and sintered using a commercial photonic curing system (PulseForge® 3300, Novacentrix, Austin, TX, USA.) [Schemes 1(c) and 1(d)]. This process was performed under ambient atmosphere at room temperature. Typical input parameters were voltage (220 V) and pulse duration (1400 μs). The measured radiant exposure energy for each pulse was 2.4 J·cm^{-2}. Different numbers of pulses were applied to cure the ECAs. The repetition rate was 3 Hz.

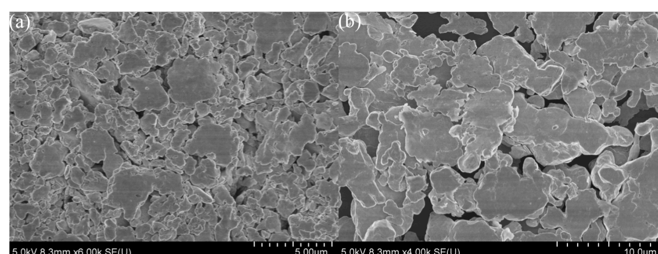

Figure 1 Surface morphologies of (a) AgC-239 and (b) AgC-224 micro silver flakes

Characterization

The structures of the samples were recorded using a PerkinElmer Frontier TN FTIR spectrophotometer (PerkinElmer, Waltham, MA, USA); 32 scans were collected at a spectral resolution of 1 cm^{-1}. The curing of the samples was studied using a NETZSCH 204 F1 DSC (NETZSCH, Selb, Germany) operated under an atmosphere of pure Ar atmosphere. The sample (*ca.* 10 mg) was placed in a sealed aluminium sample pan. The curing scans were conducted from 40 to 300 °C at a rate of 10 °C·min^{-1} under an Ar flow rate of 25 ml·min^{-1}. The thermal stabilities of the samples were measured using a NETZSCH 2000SE/H/24/1 TG-DTA analyzer (NETZSCH, Selb, Germany) operated under a pure N_2 atmosphere. The sample (*ca.* 10 mg) was placed in a Pt cell and heated at a rate of 10 °C·min^{-1} from 30 to 900 °C under a N_2 flow rate of 60 ml·min^{-1}. SEM images of the samples were recorded using a Hitachi SU8020 FE-SEM microscope (Hitachi, Tokyo, Japan) operated at an accelerating voltage of 5 kV and an accelerating current of 2 μA. The bulk resistivity of the samples was obtained using a Loresta-GP MCP-T610 resistivity meter (Mitsubishi Chemical Analytech, Co., Ltd., Kanagawa, Japan) through a four-point probe method. The tested samples were prepared according to Figure S1. The

RSC Advances Accepted Manuscript

ECAs were printed onto a glass substrate (50 mm×10 mm×1 mm) by the help of a glue tape (thickness 50 μm, 3M, Maplewood, MN, USA) to form ECAs films (30 mm×5 mm ×0.05 mm). 30 samples were tested for each value. The shear strength of the samples was obtained using a Nordson Dage Series 4000 multipurpose bondtester (Nordson, Westlake, OH, USA) through a DS 100 kg SK Chipshear model. The tested samples were prepared according to Figure S2. The printed ECAs film (5 mm×5 mm×0.05 mm) onto a glass substrate (5 mm×5 mm×1 mm) was connected to another glass chip (5 mm×5 mm×1 mm) to form a sandwich structure. The width of the pusher head was 4 mm. The push rate was 100 $\mu m \cdot s^{-1}$. 30 samples were tested for each value. The optical absorption of the samples was carried out on a JASCO V-670 UV-VIS-NIR spectrophotometer (JASCO Corporation, Tokyo, Japan) in the range of 200—900 nm. The nano dynamic mechanical properties of the samples were obtained using a Hysitron TI 950 TriboIndenter (HYSITRON, Eden Prairie, MN, USA) under a scanning rate of 0.5 Hz, a tip velocity of 40 $\mu m \cdot s^{-1}$, a scanning size of 40 μm, a setpoint of 3 μN, and an integral grain of 120.

Results and discussion

Curing

We used FTIR to characterize the structures of ECAs-80. As arrowed in Figure 2, the strong sharp absorption peak at 1720 cm^{-1} featured the stretching vibration of C=O, the weak absorption peak at 1635 cm^{-1} for the stretching vibration of C=C in alkenyl, that at 1415 cm^{-1} for the in-plane bending vibration of C—H in alkenyl, and those at 985 and 805 cm^{-1} for the out-plane bending vibration of C—H in alkenyl. The cured and uncured ECAs-80 both contained these groups.

In this study, the matrix resin and micro silver flakes showed excellent light-absorbing properties. Both presented strong, sharp absorption peaks in the wavelength of 200—300 nm on UV-VIS-NIR spectra (Figure S3). Under intense pulsed light, ECAs-80 absorbed the heat produced from light, which was then transferred to the whole matrix resin system. During transferring, heat opened the double bonds at the end of molecular chains and caused them into crosslinking to accomplish curing process. In the irradiating and sintering, the temperature caused by the intense pulsed light could be up to 200 °C, which accelerated the opening and crosslinking processes. Therefore, the intense pulsed light, combined with high radiant exposure energy (2.38 $J \cdot cm^{-2}$) and long pulse duration (1400 μs), had given enough activation energy to the matrix resin and open the double end bonds to initialize the crosslinking, polymerization, and curing[49-51] [Schemes 1(d), 1(e), and 1(f)].

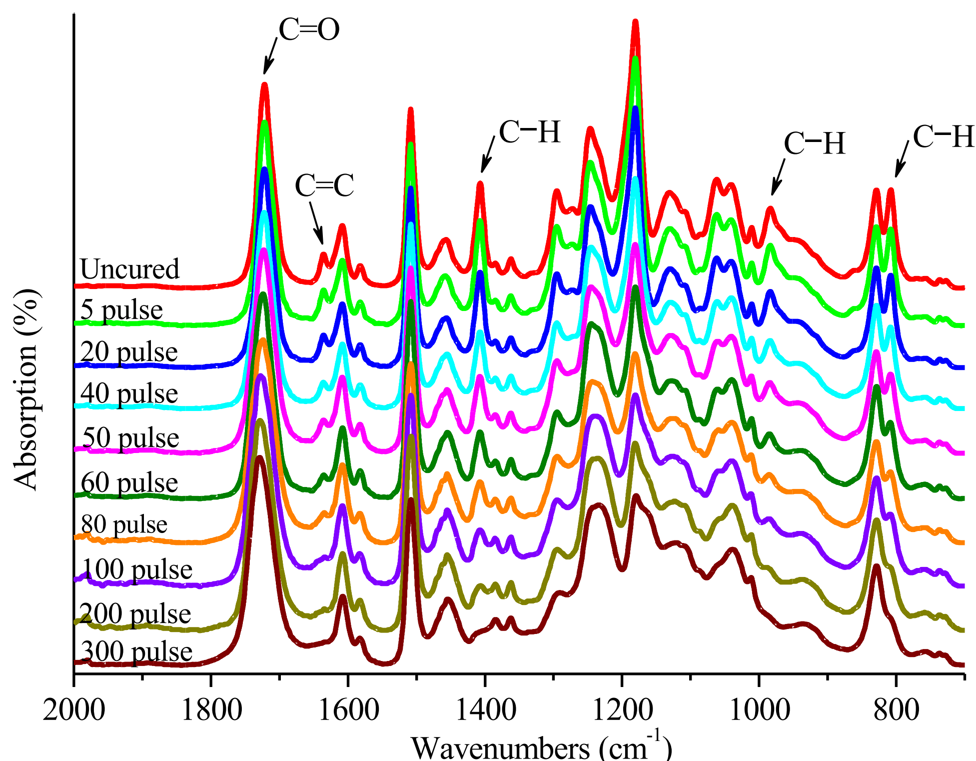

Figure 2 FTIR spectra of ECAs-80

RSC Advances Accepted Manuscript

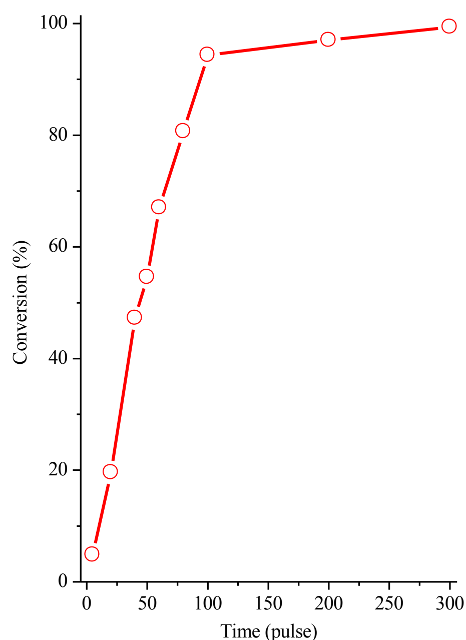

Figure 3 Double bond conversion of ECAs-80

As the number of light pulses increased from 5 to 300 pulses, the absorption peaks at 1635, 1415, 985, and 805 cm^{-1}, which represented the characteristics of alkenyl in matrix resin, became weak, and ultimately disappeared. These variations indicated that the conversion process of double bonds in the curing. The double bond conversion can be calculated using the following equation:[52-54]

$$Conversion = (1 - \frac{A^{t}_{C=C} A^{0}_{C=O}}{A^{0}_{C=C} A^{t}_{C=O}}) \times 100$$

where $A^{0}_{C=C}$ is the area of C=C absorption peak of uncured samples, $A^{t}_{C=C}$ is the area of C=C absorption peak of samples cured for a time of t, $A^{0}_{C=O}$ is the area of C=O absorption peak of uncured samples, $A^{t}_{C=O}$ is the area of C=O absorption peak of samples cured for a time of t. In the above calculation, we used the areas of C=O absorption peaks as references, because the C=O did not have any reactions during curing and often showed strong and sharp absorption peaks on FTIR spectra.

Figure 3 shows the double bond conversion of ECAs-80 vs curing time. They were 4.87% (5 pulse), 15.59% (20 pulse), 47.24% (40 pulse), 54.57% (50 pulse), 67.02% (60 pulse), 80.68% (80 pulse), 94.36% (100 pulse), 97.01% (200 pulse), and 99.38% (300 pulse), respectively. The double conversion increased sharply from 5 to 100 pulses, then showed a slow increasing trend from 200 to 300 pulses. This suggested that ECAs-80 could be cured well at 100 pulses.

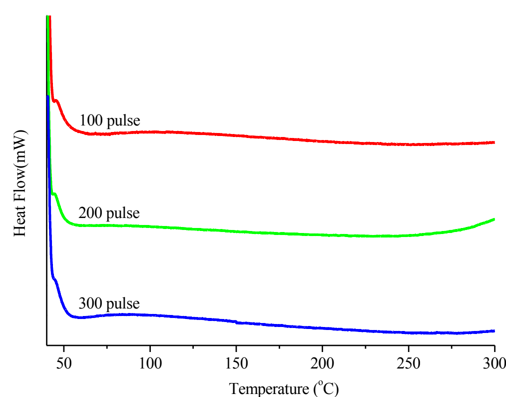

Figure 4 DSC curves of photonically cured ECAs-80

In addition, we also used DSC to characterize the curing degree of the photonic curing. As Figure 4 shows, the ECAs-80, photonically cured at 100, 200, and 300 pulses, did not present any endothermic peak within the testing temperatures (40—300 °C). This indicated the ECAs were cured well at these pulses, corresponding to the curing time of 140, 280, and 420 ms, respectively, which also coincided well the aforementioned FTIR results.

Figure 5 displays the TG-DTA traces of cured ECAs-80, ECAs-85, and ECAs-90. As Figure 5(a) shows, the TG traces revealed the loss of matrix resin; the total weight loss was about 17% (ECAs-80, 100 pulse), 14% (ECAs-85, 100 pulse), 10% (ECAs-90, 100 pulse), 8% (ECAs-80, 500 pulse), 6% (ECAs-85, 500 pulse), and 4% (ECAs-90, 500 pulse) at the temperatures up to 900 °C. The weight loss increased quickly from about 350 to 450 °C, where the pyrolysis rate was the maximum. Above that, the weight loss was slow. The high pyrolysis temperature above 350 °C suggested these ECAs all had high temperature stability. The weight losses of ECAs-80, ECAs-85, and ECAs-90 at 500 pulses were less than those at 100 pulses. This is because the intense pulsed light produced too much energy in a long curing time, which caused the pyrolysis of matrix resin under atmospheric ambient.

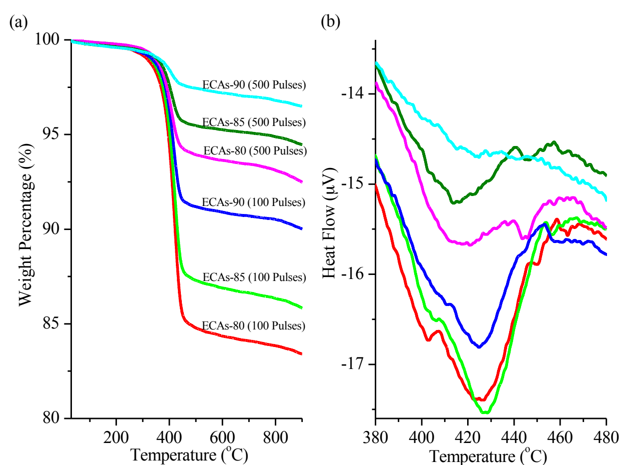

Figure 5 TG-DTA traces of ECAs-80, ECAs-85, and ECAs-90: (a) TG and (b) DTA traces

This journal is © The Royal Society of Chemistry 2012

RSC Advances Accepted Manuscript

Figure 5(b) shows the DTA traces of ECAs-80, ECAs-85, and ECAs-90 at 100 and 500 pulses. They all had an endothermic peak in the range of 350—450 °C. Apparently, the shape, intensity, and area of these endothermic peaks changed accordingly with the weight losses of ECAs-80, ECAs-85, and ECAs-90. The higher the weight loss, the sharper, stronger, and larger the endothermic peak. At 100 pulses, the weight losses of ECAs-80, ECAs-85, and ECAs-90 were approximately equal to the weight percentages of matrix resin in them, even exactly. From the weight loss and endothermic peak, it can be seen that the ECAs achieved good curing with negligible pyrolysis of matrix resin using 100 pulses irradiating and sintering energy with 140 ms under atmospheric ambient. Compared to those heat cured using 30—60 min at 120—150 °C or ultraviolet rays cured using several to tens of minutes, the intense pulsed light curing was ultra fast. Importantly, there was only one weight loss step and one endothermic peak for each ECAs, which indicated that a crosslinked homogeneous polymer had been formed from matrix resin by the intense pulsed light [Schemes 1(e) and 1(f)], with no any residual monomers or small molecules. Combing the double conversion and weight loss, we set the 100 pulses as the curing time of ECAs in this study.

Electrical properties

The samples were prepared using 100 pulses for bulk resistivity (Figure S1). Besides AgC-239 micro silver flakes, AgC-224 micro silver flakes [Figure 1(b), Fukuda Metal Foil & Powder Co., Ltd., Kyoto, Japan] had been used to fabricate ECAs for comparison samples. Figure 6 shows the bulk resistivity results. As the weight percentage of micro silver flakes increased from 80% to 90% in ECAs, the bulk resistivity decreased accordingly.

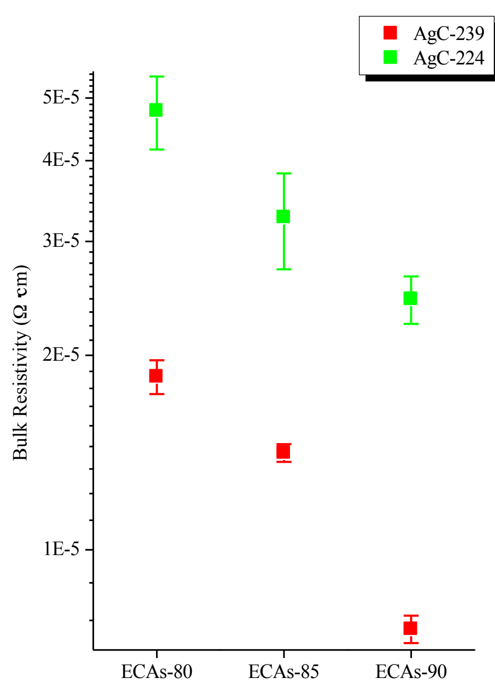

Figure 6 Bulk resistivity of ECAs-80, ECAs-85, and ECAs-90 at 100 pulses

Bulk resistivity had a close relationship to the content of electrically conductive fillers; the more the latter, the lower the former, because the increasing electrically conductive fillers formed more electrically conductive channels, which decreased the bulk resistivity. AgC-239 micro silver flakes had a more significant effect on decreasing bulk resistivity than AgC-224 micro silver flakes. As Figure 6 shows, the bulk resistivity was 1.85×10^{-5}, 1.41×10^{-5}, and 7.54×10^{-6} Ω·cm, respectively, for ECAs-80, ECAs-85, and ECAs-90 fabricated from AgC-239 micro silver flakes, while 4.78×10^{-5}, 3.27×10^{-5} and 2.44×10^{-5} Ω·cm for those from AgC-224 micro silver flakes. In addition, the bulk resistivity values from AgC-239 micro silver flakes were also much lower than those at 3×10^{-5} to 5×10^{-5} Ω·cm in our previous studies.[6,10,11,16,17]

The formation of electrically conductive channels (also called electrically conductive networks) in ECAs mainly came from the contact points and areas between/among electrically conductive fillers; the more the contact points, the larger the contact area, and the higher the electrical conductivity. To obtain clear profiles of electrically conductive channels, the ECAs-90 from AgC-239 and AgC-224 micro silver flakes were irradiated and sintered for 500 pulses, respectively. After this process, the matrix resin was pyrolysized almost completely; there were only micro silver flakes left in ECAs. Thus, the electrically conductive channels were formed by sintered structures [Figures 7(a) and 7(b)]. Apparently, the shape and size of micro silver flakes influenced the formation of electrically conductive channels greatly. AgC-239 micro silver flakes had a size at 2—15 μm [Figure 1(a)], and AgC-224 micro silver flakes at 6—12 μm [Figure 1(b)], so that the former had a wider size distribution than the latter. Their shape was different also.

As Figure 7(a) shows, AgC-239 micro silver flakes overlapped and contacted each other to form a dense, fine electrically conductive network. The interspaces and holes between/among AgC-239 micro silver flakes were caused by the pyrolysis of matrix resin. They were very small. A similar electrically conductive network was also formed from AgC-224 micro silver flakes, but sparse and rough [Figure 7(b)]. Moreover, the interspaces and holes between/among AgC-224 micro silver flakes were very large. Figure 7(c) shows the cross-section morphology of ECAs-90 from AgC-239 micro silver flakes after 100 pulses. It can be seen that AgC-239 micro silver flakes dispersed densely and arranged tightly in matrix resin. While that of ECAs-90 from AgC-224 micro silver flakes did not like this. As Figure 7(d) shows, AgC-224 micro silver flakes dispersed in matrix resin evenly, but not so densely or tightly as AgC-239 micro silver flakes. Figures 7(e) and 7(f) present the arrangement models of AgC-239 and AgC-224 micro silver flakes in ECAs-90. The arrangement of AgC-224 micro silver flakes [Figure 7(f)] had many large interspaces and holes, representing that these micro silver flakes did not contact each other fully, either the electrically conductive channels were not well formed. Thus, the bulk resistivity showed high values. The arrangement of AgC-239 micro silver flakes was not in such case [Figure 7(e)]. Small micro silver flakes filled or embedded into the interspaces and holes formed by large ones, to produce many contact points and increase contact areas. By the help of this arrangement, electrically conductive channels were well formed leading to low bulk resistivity.

RSC Advances Accepted Manuscript

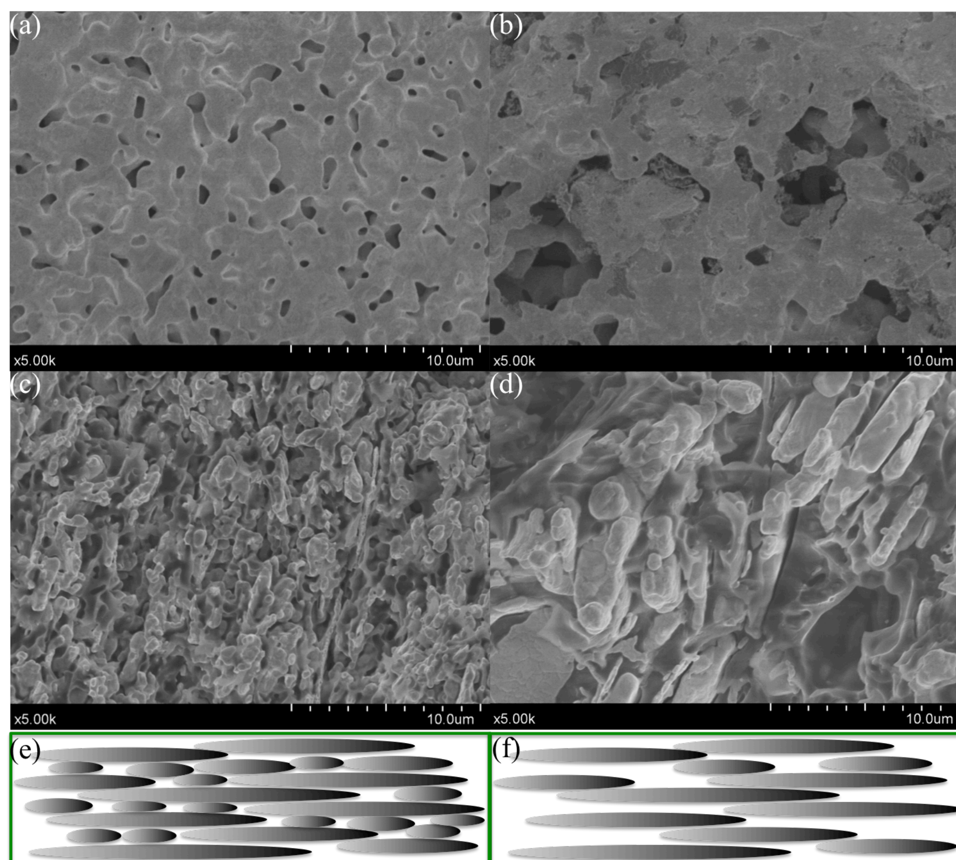

Figure 7 Surface morphologies of sintered structure of ECAs-90 (500 pulses) with (a) AgC-239 and (b) AgC-224 micro silver flakes, cross-section morphology of ECAs-90 (100 pulses) with (c) AgC-239 and (d) AgC-224 micro silver flakes, and arrangement model of (e) AgC-239 and (f) AgC-224 micro silver flakes in ECAs-90

Mechanical properties

To investigate the mechanical properties of photonic curing ECAs, the samples for shear test were designed according to Figure S2. ECAs were printed onto a glass substrate, and then a glass chip was put on the ECAs film to form a sandwich structure. As described above, the 0.05 mm thick ECAs film was cured well by direct exposure to intense pulsed light for 100 pulses. During the preparation of shear-test samples, the intense pulsed light at 100 pulses could not cure the sandwiched ECAs film entirely because glass chip covered and weakened the light intensity greatly. To fully cure the ECAs films in these samples, 500 pulses were used.

Figure 8(a) presents the shear strength of ECAs-80, ECAs-85, and ECAs-90 obtained from shear test. These shear strength values at 6.75, 6.25, and 5.00 MPa were higher than some previously reported results at 4－11 MPa.[6,10,11,33,34] The intense pulsed light, combining of high bank voltage (220 V), long pulse duration (1400 μs), and high radiant exposure energy (2.38 $J\cdot cm^{-2}$), had been used to cure these ECAs. Matrix resin and micro silver flakes firstly absorbed the light and the heat produced from light, which were then transferred into the whole matrix resin system [Figure 8(b)]. With the heat, the double bonds at the end of molecular chains were initialized into crosslinking and polymerization, and then cured ECAs as reported.[51-54] The process also caused the pyrolysis of matrix resin and sintered micro silver flakes together [Figures 7(a) and 7(b)].

Matrix resin connected together via opened double bond and crosslinked into macromolecules as FTIR spectra reflected. Moreover, the main molecular chains of matrix resin contained hydroxyl, carbonyl, and epoxy groups. They were induced to form intermolecular hydrogen bonds [Figure S4(a)]. In addition, hydrogen bonds were also formed between AgC-239 micro silvers and crosslinked macromolecules of bisphenol A epoxy acrylate [Figure S4(b)] and ethoxylated bisphenol A diacrylate [Figure S4(c)], because the coated fatty acid on micro silver flakes had these functional groups, too. In a word, good curing, sintered micro silver flakes, and hydrogen bonds all gave contributions to the high shear strength of photonically cured ECAs.

It also can be seen that the mechanical strength of ECAs were reduced with increasing micro silver flakes content due to cutting off the crosslinked structures within the matrix resin. Figure 9 presents the surface morphologies of pushed fracture interfaces on glass substrates and chips. The pushed fracture interfaces on glass substrates all looked flat. Those at ECAs-80 had the most collapses and potholes [Figure 9(a)], ECAs-85 followed [Figure 9(c)], and ECAS-90 final with few collapses and potholes [Figure 9(e)]. The pushed fracture interfaces on glass chips were made up of torn particles, torn traces, collapses, and potholes, showing a decreasing rough state from ECAs-80 [Figure 9(b)] to ECAs-85 [Figure 9(d)], and to ECAs-90 [Figure 9(f)].

RSC Advances Accepted Manuscript

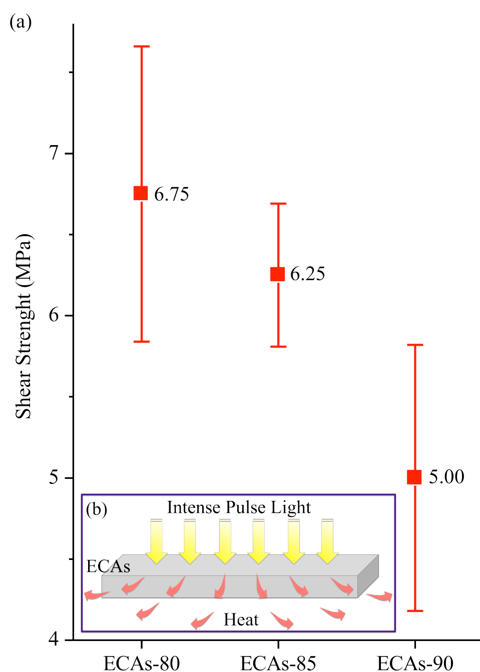

Figure 8 (a) shear strength of ECAs-80, ECAs-85, and ECAs-90 from photonic curing (500 pulses) and (b) light and heat transferring diagram

In short, the sandwiched ECAs films were cracked from side to side, from glass substrate (bonding interface) to glass chip (bonded interface), to form these surface morphologies. The pushed fracture interfaces on glass chips were much rougher than those on glass substrates. The surface roughness decreased visually as the weight percentage of micro silver flakes increased from 80% to 90%. Moreover, solid-to-solid contacts among glass substrate, ECAs, and glass chip increased accordingly as micro silver flakes increased in ECAs, which also reduced the mechanical strength. Because of the variations of surface morphology, surface roughness, and solid-to-solid contact, the shear strength of ECAs decreased as the weight percentage of micro silver flakes increased from 80% to 90% in ECAs [Figure 8(a)].

We also used nanoindentation to study the nano dynamic mechanical properties of ECAs. The photonically cured ECAs-80 at 100 pulses (Figure S1) was polished mechanically using an ECOMET 300 variable speed grinder-polisher (Buehler, Lake Bluff, IL, USA). Figure S5 presents the polished cross-section of samples. The thickness of cured ECAs film was about 50 μm on glass substrate. The storage and loss moduli at different depths in the ECAs film were obtained using a nanoindentation technique. As Figure 10(a) shows, the storage modulus at a position of 0—32 μm was for ECAs, and that at 32—40 μm for glass substrate. In the range of 0—32 μm, matrix resin showed a low storage modulus around 7 GPa at positions of 7—14, 16—17, 22—24, and 27—32 μm; other storage modulus peaks in this range were caused by micro

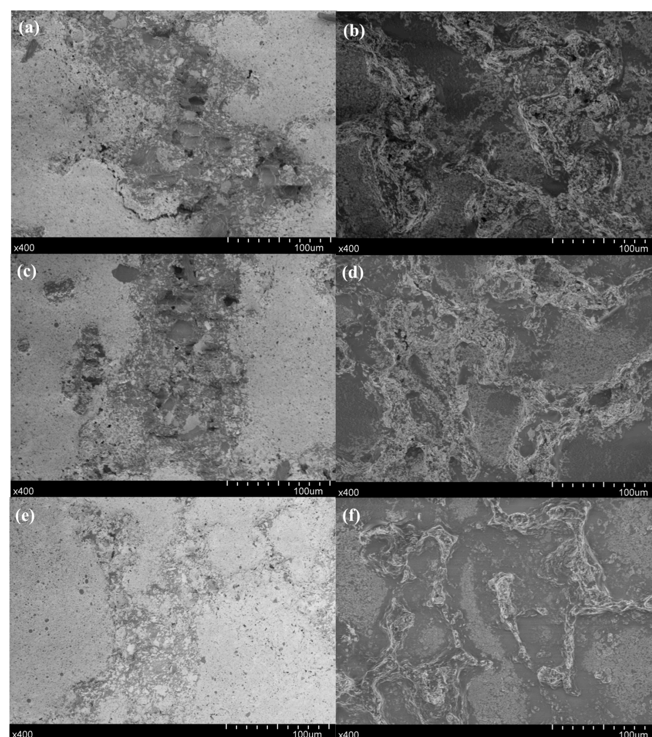

Figure 9 Surface morphology: (a), (c), and (e) pushed fracture interfaces on glass substrates, (b), (d), and (f) pushed fracture interfaces on glass chips; (a) and (b) bonded by ECAs-80, (c) and (d) by ECAs-85, (e) and (f) by ECAs-90

silver flakes [Figure 10(b)]. Figure 10(c) shows the loss storage modulus. As same as storage modulus, micro silver flakes also caused the loss modulus peaks in the range of 0—32 μm [Figure 10(d)]; matrix resin displayed a low loss modulus around 1.9 GPa, and that at 32—40 μm was for glass substrate. Matrix resin presented same storage and loss moduli at different positions (or depths), as the dash lines marked in Figures 10(a) and 10(c). This phenomenon also suggested that these ECAs were crosslinked and cured uniformly at 100 pulses, which coincided well with FTIR spectra (Figure 2), double conversion (Figure 3), DSC curves (Figure 4), and TG-DTA traces (Figure 5).

Furthermore, the ECAs fabricated in this study were stored at room temperature avoiding light. There was no gel, separation, delamination, or curing during the storing. They had a storage time as long as that of matrix resin, which were far superior to those existing ECAs products needing frozen storage. With the ultra fast curing under intense pulsed light, low bulk resistivity, high mechanical strength, long storage time at room temperature, no any other additives, and easily used, these ECAs are bound to have a good application prospect in printed electronics, which need low temperature and fast speed processes.

RSC Advances Accepted Manuscript

This journal is © The Royal Society of Chemistry 2012

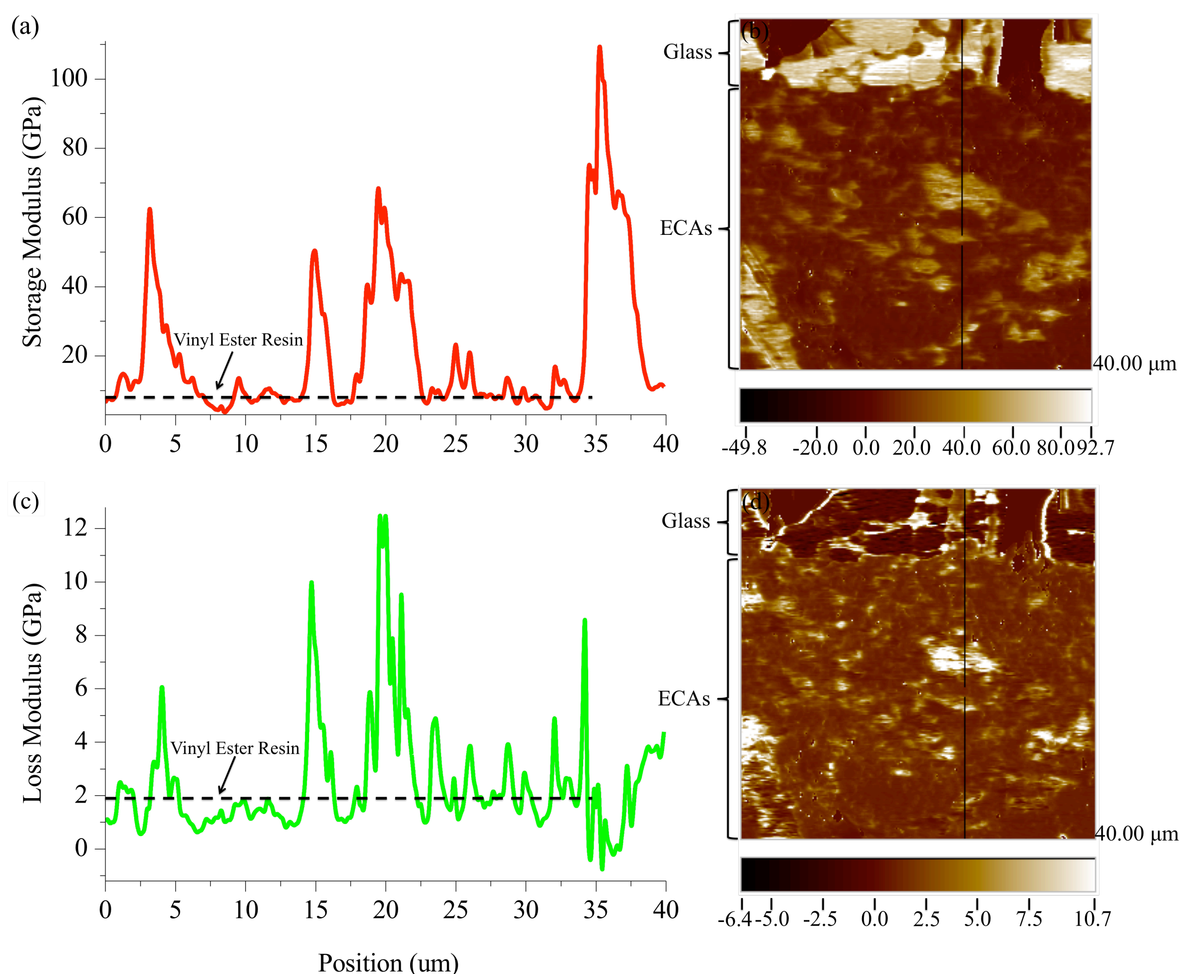

Figure 10 (a) storage modulus, (c) loss modulus, (b) and (d) tested cross-sections of photonically cured ECAs-80 (100 pulse)

Conclusions

In this study, we introduced the photonic curing process to cure the ECAs fabricated from a vinyl ester resin and micro silver flakes. Conventional heat curing at 120—150 °C in 30—60 min and ultraviolet ray curing takes several to tens of minutes. In contrast, this process can be completed in only 140 ms without any photo sensitizer or photo initiator. The vinyl ester resin/silver flakes electrically conductive adhesives absorbed the intense pulsed light and opened the double bonds in the resin resulting in crosslinking and curing. When the weight percentages of micro silver flakes were 80%, 85%, and 90% in ECAs, the bulk resistivity was at 1.85×10^{-5}, 1.41×10^{-5}, and 7.54×10^{-6} Ω·cm, and the shear strength at 6.75, 6.25, and 5.00 MPa, which were good enough for the application in printed electronic field. These ECAs with low bulk resistivity, high mechanical strength, and long storage time have been formed using photonic curing at room temperature and ambient atmosphere, which will be used to manufacture electronic devices in the future.

Acknowledgements

The authors are very grateful to Dr. Naoki Fujisawa (Hysitron Inc.) for assistance with nanoindentation measurements.

Notes and references

[a] Institute of Scientific and Industrial Research, Osaka University, Mihogaoka 8-1, Ibaraki, Osaka 567, Japan;
E-mail address: cuihuiwang@eco.sanken.osaka-u.ac.jp, cuihuiwang@hotmail.com.
[b] Institute for Polymers and Chemicals Business Development Center, Showa Denko K. K., 5-1 Yawata Kaigan Dori, Ichihara, Chiba 290-0067, Japan.
[c] NCC Nano, LLC, 200-B Parker Drive, Suite 580, Austin, TX 78728, USA.

† Electronic Supplementary Information (ESI) available: [Diagrams and UV-VIS-NIR spectra]. See DOI: 10.1039/b000000x/

RSC Advances Accepted Manuscript

1 Y. Li, K.S. Moon and C.P. Wong, *Science*, 2005, **308**, 1419-1420.
2 D. Lu and C.P. Wong. Conductive adhesives for flip-chip applications. In: Advanced Flip Chip Packaging, H.M. Tong, Y.S. Lai and C.P. Wong (eds.), Springer, New York, US, 2013, pp. 201-261.
3 L.N. Ho and H. Nishikawa, *J. Electron. Mater.*, 2012, **41**, 2527-2532.
4 X.Y. Zhu, Y.L. Liu, J.M. Long and X.L. Liu, *Rare Met.*, 2012, **31**, 64-70.
5 F.T. Tan, X.L. Qiao, J.G. Chen and H.S. Wang, *Int. J. Adhes. Adhes.*, 2006, **26**, 406-413.
6 H.W. Cui, Q. Fan, D.S. Li and X. Tang, *J. Adhes.*, 2013, **89**, 19-36.
7 X.J. Yang, W. He, S.X. Wang, G.Y. Zhou and Y. Tang, *J. Mater. Sci.-Mater. Electron.*, 2012, **23**, 108-114.
8 G.Y. Si, Y.H. Zhao, J.T. Lv, M.Q. Lu, F.W. Wang, H.L. Liu, N. Xiang, T.J. Huang, A.J. Danner, J.H. Teng and Y.J. Liu, *Nanoscale*, 2013, **5**, 6243-6248.
9 Y. Kwon, B.S. Yim, J.M. Kim and J. Kim, *Microelectron. Reliab.*, 2011, **51**, 812-818.
10 H.W. Cui, A. Kowalczyk, D.S. Li and Q. Fan, *Int. J. Adhes. Adhes.*, 2013, **44**, 220-225.
11 H.W. Cui, D.S. Li and Q. Fan, *Electron. Mater. Lett.*, 2013, **9**, 299-307.
12 Y. Zhang, S.H. Qi, X.M. Wu and G.C. Duan, *Synthetic Met.*, 2011, **161**, 516-522.
13 J. Tang, Q. Chen, L.G. Xu, S. Zhang, L.Z. Feng, L. Cheng, H. Xu, Z. Liu and R. Peng, *ACS Appl. Mater. Interf.*, 2013, **5**, 3867-3874.
14 Z.X. Zhang, X.Y. Chen and F. Xiao, *J. Adhes. Sci. Technol.*, 2011, **25**, 1465-1480.
15 J.T. Jiu, M. Nogi, T. Sugahara, T. Tokuno, T. Araki, N. Komoda, K. Suganuma, H. Uchida and K. Shinozaki, *J. Mater. Chem.*, 2012, **22**, 23561-23567.
16 H.W. Cui, D.S. Li and Q. Fan, *Electron. Mater. Lett.*, 2013, **9**, 1-5.
17 H.W. Cui, D.S. Li, Q. Fan and H.X. Lai, *Int. J Adhes. Adhes.*, 2013, **44**, 232-236.
18 M. Inoue, H. Muta, S. Yamanaka and K. Suganuma, *J. Electron. Mater.*, 2009, **38**, 2013-2022.
19 Z. Li, K. Hansen, Y.G. Yao, Y.Q. Ma, K.S. Moon and C.P. Wong, *J. Mater. Chem. C*, 2013, **1**, 4368-4374.
20 M. Yoonessi, D.A. Scheiman, M. Dittler, J.A. Peck, J. Ilavskye, J.R. Gaierc and M.A. Meador, *Polymer*, 2013, **54**, 2776-2784.
21 X.H. Zhong, R. Wang and Y.Y. Wen, *Phys. Chem. Chem. Phys.*, 2013,**15**, 3861-3865.
22 Q. Yin, A.J. Li, W.Q. Wang, L.G. Xia and Y.M. Wang, *J. Power Sources*, 2007, **165**, 717-721.
23 N.L. Liu, S.H. Qi, S.S. Li, X.M. Wu and L.M. Wu, *Polym. Test.*, 2011, **30**, 390-396.
24 T. Araki, M. Nogi, K. Suganuma, M. Kogure and O. Kirihara, *IEEE Electron. Device Lett.*, 2011, **32**, 1424-1426.
25 T. Araki, T. Sugahara, M. Nogi and K. Suganuma, *Jpn. J. Appl. Phys.*, 2012, **51**, 11PD01.
26 R. Abderrahmen, C. Gavory, D. Chaussy, S. Briançon, H. Fessi and M.N. Belgacem, *Int. J. Adhes. Adhes.*, 2011, **31**, 629-633.
27 Z. Czech, A. Kowalczyk, R. Pełech, R.J. Wróbelb, L. Shao, Y. Bai and J. Świdersk, *Int. J. Adhes. Adhes.*, 2012, **36**, 20-24.
28 H.W. Cui and W.H. Du, *J. Adhes.*, 2013, **89**, 714-726.
29 W.T. Xu and S.W. Rhee, *Org. Electron.*, 2010, **11**, 996-1004.
30 J.C. Zhao, F.P. Du, X.P. Zhou, W. Cui, X.M. Wang, H. Zhu, X.L. Xie and Y.W. Mai, *Compos. Part B-Eng.*, 2011, **42**, 2111-2116.
31 H.Y. Li, K.S. Moon and C.P. Wong, *J. Electron. Mater.*, 2004, **33**, 106-113.
32 J. Lee, C.S. Cho and J.E. Morris, *Microsyst. Technol.*, 2009, **15**, 145-149.
33 H.W. Cui, D.S. Li and Q. Fan, *Polym. Adv. Technol.*, 2013, **24**, 114-117.
34 H.W. Cui, Q. Fan and D.S. Li, *Polym. Int.*, 2013, **62**, 1644-1651.
35 Y. Li, D. Lu and C.P. Wong, Characterizations of electrically conductive adhesives. In: Electrical Conductive Adhesives with Nanotechnologies, Y. Li, D. Lu and C.P. Wong (eds.), Springer, New York, US, 2010, pp. 81-120.
36 W.T. Cheng, Y.W. Chih and C.W. Lin, *Int. J. Adhes. Adhes.*, 2007, **27**, 236-243.
37 Y. Zhang, S.H. Qi, X.M. Wu and G.C. Duan, *Synthetic Met.*, 2011, **161**, 516-522.
38 M. Allen, M. Aronniemi, T. Mattila, A. Alastalo, K. Ojanperä, M. Suhonen and H. Seppä, *Nanotechnology*, 2008, **19**, 175201.
39 J. Leppäniemi, M. Aronniemi, T. Mattila, A. Alastalo, M. Allen and H. Seppä, *IEEE Trans. Electron. Device*, 2011, **58**, 151-159.
40 K. Maekawa, K. Yamasaki, T. Niizeki, M. Mita, Y. Matsuba, N. Terada and H. Saito, *IEEE Trans. Compon. Pack. Manuf. Technol.*, 2012, **2**, 868-877.
41 K. Zimmer, M. Ehrhardt, P. Lorenz, T. Stephan, R. Ebert and A. Braun, *Opt. Laser Technol.*, 2013, **49**, 320-324.
42 J. Perelaer, M. Klokkenburg, C.E. Hendriks and U.S. Schubert, *Adv. Mater.*, 2009, **21**, 4830-4834.
43 J. Perelaer, R. Abbel, S. Wünscher, R. Jani, T. van Lammeren and U.S. Schubert, *Adv. Mater.*, 2012, **24**, 2620-2625.
44 K.A. Schroder, S.C. McCool and W.R. Furlan, *Technical Proceedings of the 2006 NSTI Nanotechnology Conference and Trade Show*, 2006, **3**, 198-201.
45 K.A. Schroder, *Technical Proceedings of the 2011 NSTI Nanotechnology Conference and Trade Show*, 2011, **2**, 220-223.
46 W.H. Chung, H.J. Hwang, S.H. Lee and H.S. Kim, *Nanotechnology*, 2013, **24**, 035202.
47 S.H. Park, S. Jang, D.J. Lee, J. Oh and H.S. Kim, *J. Micromech. Microeng.*, 2013, **23**, 015013.
48 H.S. Kim, S.R. Dhage, D.E. Shim and H.T. Hahn, *Appl. Phys. A*, 2009, **97**, 791-798.
49 J.S. Kang, J. Ryu, H.S. Kim and H.T. Hahn, *J. Electron. Mater.*, 2011, **40**, 2268-2277.
50 B.Y. Wang, T.H. Yoo, Y.W. Song, D.S. Lim and Y.J. Oh, *ACS Appl. Mater. Interf.*, 2013, **5**, 4113-4119.
51 Q.J. Mao, L.J. Bian and M. Huang, *J. Polym. Res.*, 2011, **18**, 1751-1756.
52 L. Jin, T. Agag and H. Ishida, *Polym. Int.*, 2013, **62**, 71-78.
53 A. Mautner, X.H. Qin, H. Wutzel, S.C. Ligon, B. Kapeller, D. Moser, G. Russmueller, J. Stampfl and R. Liska, *J. Polym. Sci. Part A-Polym. Chem.*, 2013, **51**, 203-212.
54 J.Z.Y. Wang and R.H. Bogner, *Int. J. Pharm.*, 1995, **113**, 113-122.

RSC Advances Accepted Manuscript